Journal of Organometallic Chemistry 693 (2008) 3613–3621

Contents lists available at ScienceDirect

Journal of Organometallic Chemistry

journal homepage: www.elsevier.com/locate/jorganchem

A comparative study of the reactivity of unsaturated triosmium clusters $[Os_3(CO)_8\{\mu_3\text{-}Ph_2PCH_2P(Ph)C_6H_4\}(\mu\text{-}H)]$ and $[Os_3(CO)_9\{\mu_3\text{-}\eta^2\text{-}C_7H_3(2\text{-}Me)NS\}(\mu\text{-}H)]$ with ^{t}BuNC

Arun K. Raha [a], Shishir Ghosh [a], Md. Manzurul Karim [a], Derek A. Tocher [b], Noorjahan Begum [c], Ayesha Sharmin [d], Edward Rosenberg [d], Shariff E. Kabir [a,*]

[a] Department of Chemistry, Jahangirnagar University, Savar, Dhaka 1342, Bangladesh
[b] Department of Chemistry, University College London, 20 Gordon Street, London WC1H OAJ, UK
[c] Department of Agricultural Chemistry, Sher-e-Bangla Agricultural University, Sher-e-Bangla Nagar, Dhaka 1207, Bangladesh
[d] Department of Chemistry, The University of Montana, Missoula, MT 59812, USA

ARTICLE INFO

Article history:
Received 6 August 2008
Received in revised form 24 August 2008
Accepted 25 August 2008
Available online 31 August 2008

Keywords:
Unsaturated clusters
Diphosphine
2-Methylbenzothiazole
tert-Butyl isocyanide
X-ray structures

ABSTRACT

Treatment of unsaturated $[Os_3(CO)_8\{\mu_3\text{-}Ph_2PCH_2P(Ph)C_6H_4\}(\mu\text{-}H)]$ (**2**) with ^{t}BuNC at room temperature gives $[Os_3(CO)_8(CNBu^t)\{\mu_3\text{-}Ph_2PCH_2P(Ph)C_6H_4\}(\mu\text{-}H)]$ (**3**) which on thermolysis in refluxing toluene furnishes $[Os_3(CO)_7(CNBu^t)\{\mu_3\text{-}Ph_2PCHP(Ph)C_6H_4\}(\mu\text{-}H)_2]$ (**4**). Reaction of the labile complex $[Os_3(CO)_9(\mu\text{-dppm})(NCMe)]$ (**5**) with ^{t}BuNC at room temperature affords the substitution product $[Os_3(CO)_9(\mu\text{-dppm})(CNBu^t)]$ (**6**). Thermolysis of **6** in refluxing toluene gives **4**. On the other hand, the reaction of unsaturated $[Os_3(CO)_9\{\mu_3\text{-}\eta^2\text{-}C_7H_3(2\text{-}Me)NS\}(\mu\text{-}H)]$ (**7**) with ^{t}BuNC yields the addition product $[Os_3(CO)_9(CNBu^t)\{\mu\text{-}\eta^2\text{-}C_7H_3(2\text{-}Me)NS\}(\mu\text{-}H)]$ (**8**) which on decarbonylation in refluxing toluene gives unsaturated $[Os_3(CO)_8(CNBu^t)\{\mu_3\text{-}\eta^2\text{-}C_7H_3(2\text{-}Me)NS\}(\mu\text{-}H)]$ (**9**). Compound **9** reacts with PPh_3 at room temperature to give the adduct $[Os_3(CO)_8(PPh_3)(CNBu^t)\{\mu\text{-}\eta^2\text{-}C_7H_3(2\text{-}Me)NS(\mu\text{-}H)]$ (**10**). Compound **8** exists as two isomers in solution whereas **10** occurs in four isomeric forms. The molecular structures of **3**, **6**, **8**, and **10** have been determined by X-ray diffraction studies.

1. Introduction

It is well known that coordinatively unsaturated transition metal cluster complexes, are much more reactive relative to their electron precise counterparts [1–3]. Electron-deficiency in these clusters makes them more vulnerable to attack by nucleophiles. Furthermore, the cluster-bound ligands within these unsaturated compounds frequently interact with other substrates to give new products that are not obtainable by conventional organic synthesis [4–6]. As a consequence, these electron-deficient triosmium clusters have attracted considerable interest for many years and their chemistry has been thoroughly investigated during the last decade to reveal their catalytic potential as well as applications in organic synthesis [4–27].

One of the most interesting unsaturated triosmium clusters $[Os_3(CO)_8\{\mu_3\text{-}Ph_2PCH_2P(Ph)C_6H_4\}(\mu\text{-}H)]$ (**2**), derived from the decarbonylation of the decacarbonyl compound $[Os_3(CO)_{10}(\mu\text{-dppm})]$ (**1**), shows unique chemical properties and its reactivity with various ligands has been studied extensively (Scheme 1). For example, it reacts with CO to form first $[Os_3(CO)_9\{\mu_3\text{-}Ph_2PCH_2P(Ph)C_6H_4\}(\mu\text{-}H)]$ and finally the decacarbonyl compound **1** [7], with H_2 to form $[Os_3(CO)_8(\mu\text{-}H)_2(\mu\text{-dppm})]$ [8], with diphenylacetylene to form $[Os_3(CO)_8(PhC{\equiv}CPh)(\mu\text{-dppm})]$ [9], with phosphines (PR_3) to give $[Os_3(CO)_8(PR_3)\{\mu_3\text{-}Ph_2PCH_2P(Ph)C_6H_4\}(\mu\text{-}H)]$ and $[Os_3(CO)_8(PR_3)_2(\mu\text{-dppm})]$ [10,11], with R_3SiH to form $[Os_3(CO)_9(SiR_3)(\mu\text{-dppm})(\mu\text{-}H)]$ and $[Os_3(CO)_7(SiR_3)\{\mu_3\text{-}Ph_2PCH_2P(Ph)C_6H_4\}(\mu\text{-}H)_2]$ [12], and with $[Au(PPh_3)]PF_6$ and HBF_4 to form the cationic clusters $[Os_3(CO)_8\{\mu_3\text{-}Ph_2PCH_2P(Ph)C_6H_4\}(\mu\text{-AuPPh}_3)(\mu\text{-}H)]PF_6$ and $[Os_3(CO)_9\{\mu_3\text{-}Ph_2PCH_2P(Ph)C_6H_4\}(\mu\text{-}H)_2]BF_4$, respectively [13].

On the other hand, the reactions of the electron-deficient benzoheterocyclic triosmium clusters of the type $[Os_3(CO)_9(\mu\text{-}H)(\mu_3\text{-}\eta^2\text{-L-}H)]$ (L = quinoline, quinoxaline, benzimidazole, benzothiazole, benzoxazole) obtained from decarbonylation of the corresponding decacabonyls $[Os_3(CO)_{10}(\mu\text{-}H)(\mu\text{-}\eta^2\text{-L-}H)]$, with neutral nucleophiles such as phosphine and amines results in ligand addition at the metal core along with rearrangements whereas reactions with anionic nucleophiles such as hydride or carbanions results in attack at the carbocyclic ring [4–6,17–20,23] (Scheme 2).

The reactivity of the dihydrido unsaturated cluster $[Os_3(CO)_{10}(\mu\text{-}H)_2]$ with isocyanides have been reported to give the simple adduct $[Os_3(CO)_{10}(L)(\mu\text{-}H)_2]$ (L = MeNC, ^{t}BuNC). Interestingly, ^{t}BuNC adduct exists as two isomers in solution of which the *trans* isomer was crystallographically characterized [22]. In the light of these

* Corresponding author. Tel.: +880 406 243 2592; fax: +880 406 243 2477.
E-mail address: skabir_ju@yahoo.com (S.E. Kabir).

0022-328X/$ - see front matter © 2008 Elsevier B.V. All rights reserved.
doi:10.1016/j.jorganchem.2008.08.032

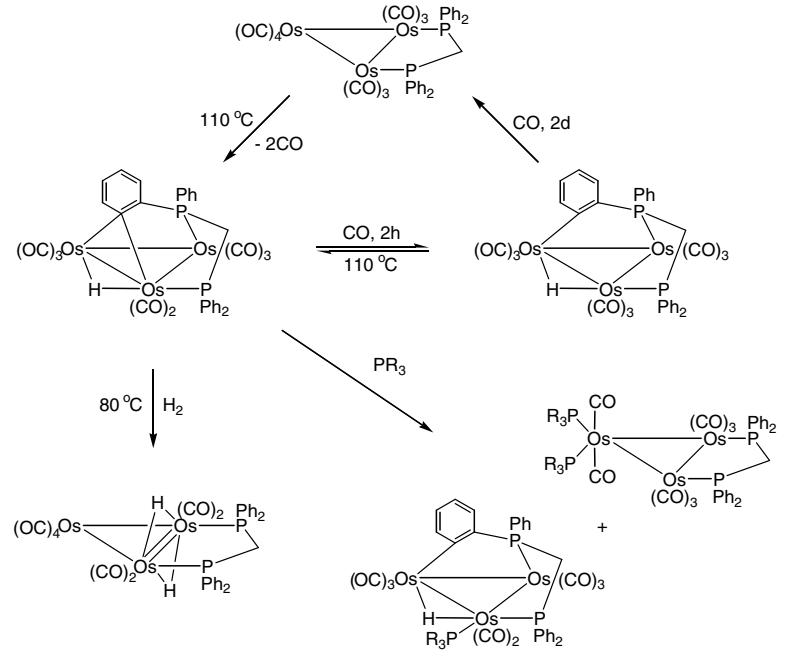

Scheme 1.

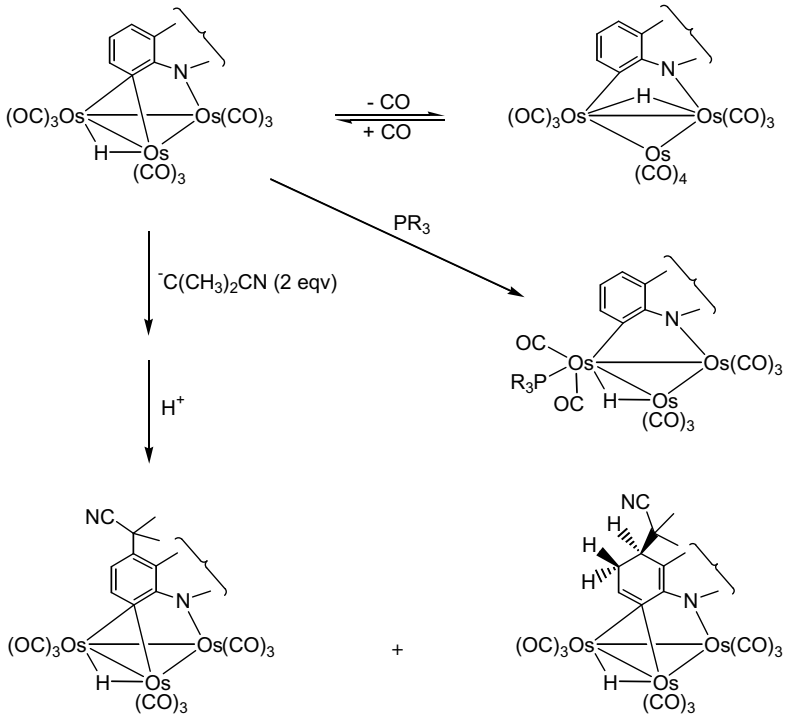

Scheme 2.

results and as an extension of our previous studies on the reactivities of these electron-deficient triosmium clusters with various organic and inorganic ligands, we have now examined the reactivity of these clusters with ^{t}BuNC and studied the effect of isocyanide–carbonyl replacement on the reactivity of the resultant complexes. These studies reveal that isocyanide coordination impacts the thermal reactivity of these two types of unsaturated triosmium clusters differently.

2. Experimental

All reactions were performed under a nitrogen atmosphere. Reagent grade solvents were dried by the standard procedures and were freshly distilled prior to use. The clusters $[Os_3(CO)_8\{\mu_3\text{-}Ph_2PCH_2P(Ph)C_6H_4\}(\mu\text{-}H)]$ (**2**) [7], $[Os_3(CO)_9(\mu\text{-dppm})(NCMe)]$ (**5**) [27] and $[Os_3(CO)_9\{\mu_3\text{-}\eta^2\text{-}C_7H_3(2\text{-}Me)NS\}(\mu\text{-}H)]$ (**7**) [20] were prepared according to the published procedures. Tert-butylisocyanide

was purchased from Strem Chemicals and used as received. Infrared spectra were recorded on a Shimadzu FTIR 8101 spectrophotometer. ^{1}H and ^{31}P-{^{1}H} NMR spectra were recorded on a Bruker DPX 400 instrument. All chemical shifts are reported in δ units with reference to the residual protons of the deuterated solvents for proton and to external 85% H_3PO_4 for ^{31}P chemical shifts. Elemental analyses were performed by Microanalytical Laboratories, University College London. Fast atom bombardment mass spectra were obtained on a JEOL SX-102 spectrometer using 3-nitrobenzyl alcohol as matrix and CsI as calibrant.

2.1. Reaction of $[Os_3(CO)_8\{\mu_3\text{-}Ph_2PCH_2P(Ph)C_6H_4\}(\mu\text{-}H)]$ (**2**) with tert-butylisocyanide

To a dichloromethane solution of **2** (100 mg, 0.085 mmol) was added a solution (10 mL) of ^{t}BuNC (14 mg, 0.17 mmol) in the same solvent over a period of 30 min. The reaction mixture was stirred at room temperature for a further 1.5 h during which time the color changed from green to yellow. The solvent was removed under reduced pressure and the residue separated by TLC on silica gel. Elution with hexane/CH_2Cl_2 (7:3, v/v) developed one major and two very minor bands. The major band afforded $[Os_3(CO)_8(CNBu^t)\{\mu_3\text{-}Ph_2PCH_2P(Ph)C_6H_4\}(\mu\text{-}H)]$ (**3**) (42 mg, 39%) as yellow crystals after recrystallization from hexane/CH_2Cl_2 at 4 °C. Anal. Calc. for $C_{38}H_{31}NO_8Os_3P_2$: C, 36.16; H, 2.48; N, 1.11. Found: C, 36.45; H, 2.69; N, 1.18%. IR (νCO, CH_2Cl_2): 2052 vs, 2015 vs, 1995 s, 1975 s, 1951 m, 1921 w cm^{-1}, (νCN, CH_2Cl_2): 2178 s cm^{-1}; ^{1}H NMR ($CDCl_3$): δ 7.99 (d, 1H, J = 5.1 Hz), 7.28–7.03 (m, 15H), 6.46 (d, 1H, J = 4.8 Hz,), 6.13 (t, 1H, J = 4.8 Hz), 6.07 (t, 1H, J = 5.1 Hz), 5.36 (m, 1H), 3.48 (m, 1H), 1.41 (s, 9H), −16.62 (d, 1H, J = 7.6 Hz); ^{31}P-{^{1}H} NMR ($CDCl_3$): δ 12.7 (d, 1P, J = 75.6 Hz,), 16.5 (d, 1P, J = 75.6 Hz); MS (FAB): m/z 1263 (M^+).

2.2. Thermolysis of $[Os_3(CO)_8(CNBu^t))\{\mu_3\text{-}Ph_2PCH_2P(Ph)C_6H_4\}(\mu\text{-}H)]$ (**3**)

A toluene solution (20 mL) of **3** (30 mg, 0.023 mmol) was heated to reflux for 2 h. The solvent was removed under reduced pressure and the residue separated by TLC on silica gel. Elution with hexane/CH_2Cl_2 developed one major and several very minor bands. The major band afforded $[Os_3(CO)_7(CNBu^t)\{\mu_3\text{-}Ph_2PCHP(Ph)C_6H_4\}\ (\mu\text{-}H)_2]$ (**4**) (13 mg, 45%) as yellow crystals from hexane/CH_2Cl_2 at −20 °C. Anal. Calc. for $C_{37}H_{31}NO_7Os_3P_2$: C, 36.00; H, 2.53; N, 1.13. Found: C, 36.32; H, 2.75; N, 1.22%. IR (νCO, CH_2Cl_2): 2057 s, 2008 vs, 1987 m, 1977 sh, 1950 m, 1938 m cm^{-1}, (νCN, CH_2Cl_2): 2183 s cm^{-1}; ^{1}H NMR ($CDCl_3$): δ 7.66 (d, 1H, J = 7.8 Hz), 7.51–6.96 (m, 15H), 6.84(t, 1H, J = 7.8 Hz), 6.72 (d, 1H, J = 7.8 Hz), 6.06 (t, 1H, J = 7.8 Hz), 5.10 (dd, 1H, J = 11.7, 4.0 Hz), 1.41 (s, 9H), −13.86 (d, 1H, J = 12.4 Hz), −16.85 (d, 1H, J = 11.2, 4.8 Hz); ^{31}P-{^{1}H} NMR ($CDCl_3$): δ −13.7 (d, 1P, J = 53.5 Hz), −61.8 (d, 1P, J = 53.5 Hz); MS (FAB): m/z 1235 (M^+).

2.3. Reaction of $[Os_3(CO)_9(\mu\text{-}dppm)(NCMe)]$ (**5**) with tert-butylisocyanide

A mixture $[Os_3(CO)_9(\mu\text{-}dppm)(NCMe)]$ (**5**) (80 mg, 0.064 mmol) and ^{t}BuNC (7 mg, 0.072 mmol) in dichloromethane (10 mL) was stirred at room temperature for 16 h. The solvent was removed *in vacuo* and the residue separated by TLC on silica gel. Elution with hexane/CH_2Cl_2 (4:1, v/v) gave three bands. The first band afforded $[Os_3(CO)_{10}(\mu\text{-}dppm)]$ (**1**) (7 mg, 9%) while the second band yielded $[Os_3(CO)_9(\mu\text{-}dppm)(CNBu^t)]$ (**6**) (42 mg, 51%) as orange crystals after recrystallization from hexane/CH_2Cl_2 at −20 °C. Anal. Calc. for $C_{36}H_{23}NO_9Os_3P_2$: C, 36.30; H, 2.42; N, 1.09. Found: C, 36.66; H, 2.65; N, 1.15%. IR (νCO, CH_2Cl_2): 2053 s, 2012 s, 1998 vs, 1980 vs, 1950 m, 1930 m cm^{-1}, (νCN, CH_2Cl_2): 2177 m cm^{-1}; ^{1}H NMR ($CDCl_3$): δ 7.66–7.19 (m, 20H), 5.05 (m, 2H), 1.48 (s, 9H); ^{31}P-{^{1}H} NMR ($CDCl_3$): δ −27.3 (s); MS (FAB): m/z 1291 (M^+).

2.4. Thermolysis of $[Os_3(CO)_9(\mu\text{-}dppm)(CNBu^t)]$ (**6**)

A toluene solution (10 mL) of **6** (25 mg, 0.019 mmol) was refluxed for 3 h. The solvent was removed under reduced pressure and the residue separated by TLC on silica gel. Elution with hexane/CH_2Cl_2 (7:3, v/v) gave two bands. The major band was identified as **4** (12 mg, 50%) and the minor band as unconsumed **6** (5 mg).

2.5. Reaction of $[Os_3(CO)_9\{\mu_3\text{-}\eta^2\text{-}C_7H_3(2\text{-}Me)NS\}(\mu\text{-}H)]$ (**7**) with ter-butylisocyanide

A dichloromethane solution (20 mL) of **7** (50 mg, 0.051 mmol) and ^{t}BuNC (14 mg, 0.17 mmol) was stirred at room temperature for 30 min during which time the color changed from green to yellow. The solvent was removed under reduced pressure and the residue separated by TLC on silica gel. Elution with hexane/CH_2Cl_2 (7:3, v/v) developed one band which afforded $[Os_3(CO)_9(CNBu^t)\{\mu\text{-}\eta^2\text{-}C_7H_3(2\text{-}Me)NS\}(\mu\text{-}H)]$ (**8**) (45 mg, 85%) as yellow crystals from hexane/CH_2Cl_2 at −4 °C. Anal. Calc. for $C_{22}H_{16}N_2O_9Os_3S$: C, 25.04; H, 1.53; N, 2.65. Found: C, 25.24; H, 1.72; N, 2.82%. IR (νCO, CH_2Cl_2): 2075 w, 2043 vs, 2029 vs, 1979 vs, cm^{-1}, (νCN, CH_2Cl_2): 2181 s cm^{-1}; ^{1}H NMR ($CDCl_3$) major isomer (95%): δ 7.97 (dd, 1H, J = 7.0, 0.6 Hz), 7.16 (dd, 1H, J = 7.0, 0.6 Hz), 6.97 (t, 1H, J = 7.0 Hz), 3.0 (s, 3H), 1.42 (s, 9H), −11.88 (s, 1H); MS (FAB): m/z 1056.

2.6. Thermolysis of $[Os_3(CO)_9(CNBu^t)\{\mu\text{-}\eta^2\text{-}C_7H_3(2\text{-}Me)NS\}(\mu\text{-}H)]$ (**8**)

A toluene solution (10 mL) of **8** (25 mg, 0.024 mmol) was heated to reflux for 3 h during which time the color changed to green. Work up followed by chromatographic separation as above afforded unreacted **8** (4 mg) and $[Os_3(CO)_8(CNBu^t)\{\mu_3\text{-}\eta^2\text{-}C_7H_3(2\text{-}Me)NS\}(\mu\text{-}H)]$ (**9**) (15 mg, %) as green crystals from hexane/CH_2Cl_2 by slow evaporation of the solvents as room temperature. Anal. Calc. for $C_{21}H_{16}N_2O_8Os_3S$: C, 25.04; H, 1.53; N, 2.65. Found: C, 25.24; H, 1.72; N, 2.82%. IR (νCO, CH_2Cl_2): 2059 vs, 2015 vs, 1993 vs, 1978 s, cm^{-1}, (νCN, CH_2Cl_2): 2164 s cm^{-1}; ^{1}H NMR ($CDCl_3$): δ 8.43(m, 1H), 8.35 (m, 1H), 6.94 (m, 1H), 2.96 (s, 3H), 1.41 (s, 9H), −12.93 (s, 1H); MS (FAB): m/z 1028.

2.7. Reaction of $[Os_3(CO)_8(CNBu^t)\{\mu_3\text{-}\eta^2\text{-}C_7H_3(2\text{-}Me)NS\}(\mu\text{-}H)]$ (**9**) with PPh_3

A dichloromethane solution (10 mL) of **9** (10 mg, 0.010 mmol) and triphenylphosphine (4 mg, 0.015 mmol) was stirred at room temperature for 30 min. The color changed from green to yellow. The solvent was removed under reduced pressure and the residue separated by TLC on silica gel. Elution with hexane developed one major and two very minor bands. The major band afforded $[Os_3(CO)_8(PPh_3)(CNBu^t)\{\mu\text{-}\eta^2\text{-}C_7H_3(2\text{-}Me)NS(\mu\text{-}H)]$ (**10**) (7 mg, 56%) as yellow crystals after recrystallization from hexane/CH_2Cl_2 at 4 °C. Anal. Calc. for $C_{39}H_{31}N_2O_8Os_3PS$: C, 36.32; H, 2.43; N, 2.17. Found: C, 36.65; H, 2.75; N, 2.32% IR (νCO, CH_2Cl_2): 2051 w, 2022 s, 1987 s, 1960 m, 1936 w, 1915 w cm^{-1}, (νCN, CH_2Cl_2): 2178 s cm^{-1}; ^{1}H NMR ($CDCl_3$) for major isomer (89%): δ 7.35 (m, 1H), 7.27–7.08 (m, 15H), 6.86 (d, 1H, J = 7.4 Hz), 6.39 (t, 1H, J = 7.4 Hz), 2.93 (s, 3H), 1.42 (s, 9H), −11.15 (d, 1H, J = 16.4 Hz); ^{31}P-{^{1}H} NMR ($CDCl_3$): δ 12.1 (s); MS (FAB): m/z 1289.

2.8. Reaction of **9** with CO

Carbon monoxide gas was bubbled through a $CDCl_3$ solution of **9** (15 mg, 0.015 mmol) in an NMR tube for 2 min. The ^{1}H NMR spectrum indicated complete conversion to cluster **8**.

2.9. X-ray structure determinations

Single crystals of **3**, **6**, **8** and **10** suitable for X-ray diffraction were grown by slow diffusion of hexane into a dichloromethane solution at 4 °C. All geometric and crystallographic data for **3**, **6**, **8** and **10** were collected at 150 K on a Bruker SMART APEX CCD diffractometer using Mo Kα radiation (λ = 0.71073 Å). Data reduction and integration was carried out with SAINT+ and absorption corrections were applied using the program SADABS [28]. Structures were solved by direct methods and developed using alternating cycles of least-squares refinement and difference-Fourier synthesis. All non-hydrogen atoms were refined anisotropically. Hydrogen atoms were placed in the calculated positions and their thermal parameters linked to those of the atoms to which they were attached (riding model). The SHELXTL PLUS V6.10 program package was used for structure solution and refinement [29]. Final difference maps did not show any residual electron density of stereochemical significance. The details of the data collection and structure refinement are given in Table 1.

3. Results and discussion

3.1. Reaction of electron-deficient $[Os_3(CO)_8\{\mu_3\text{-}Ph_2PCH_2P(Ph)C_6H_4\}(\mu\text{-}H)]$ (2) with ^{t}BuNC

Reaction of the unsaturated cluster **2** with ^{t}BuNC at room temperature, followed by the usual workup and chromatographic separation, furnishes $[Os_3(CO)_8(CNBu^t)\{\mu_3\text{-}Ph_2PCH_2P(Ph)C_6H_4\}(\mu\text{-}H)]$ (**3**) in 39% yield which decarbonylates at 110 °C to give $[Os_3(CO)_7(CNBu^t)\{\mu_3\text{-}Ph_2PCHP(Ph)C_6H_4\}(\mu\text{-}H)_2]$ (**4**) in 45% yield (Scheme 3). Compound **3** is an adduct of **2** and ^{t}BuNC whereas compound **4** represents a rare example in which activation of both aromatic and aliphatic C–H bonds has occurred. There is no evidence for the formation of $[Os_3(CO)_8(CNBu^t)_2(\mu\text{-dppm})]$ although such a disubstituted product was expected by further addition of second molecule of ^{t}BuNC ligand to **3** followed by reductive elimination of the orthometallated phenyl ring of the dppm ligand. Both compounds have been characterized by IR, ^{1}H and ^{31}P-{^{1}H} NMR, mass spectroscopy and elemental analysis together with single crystal X-ray diffraction studies for **3**.

An ORTEP diagram of the molecular structure of **3** is depicted in Fig. 1, and selected bond distances and angles are listed in the caption. Compound **3** consists of an approximate isosceles triangle of osmium atoms with one long {Os(1)–Os(3) = 3.0546(3) Å} and two shorter bonds {Os(1)–Os(2) = 2.8961(3) and Os(2)–Os(3) = 2.8714(3) Å}. The eight carbonyl ligands are all terminal, three of which are bonded to each of Os(2) and Os(3) while the other two bonded to Os(1). The ^{t}BuNC ligand is axially coordinated to Os(1) and lies on the opposite side of the Os_3 plane with respect to the μ_3-$Ph_2PCH_2P(Ph)C_6H_4$ ligand. The addition of this ligand to the unsaturated cluster **2** changes the coordination mode of the orthometallated phenyl ring. The bridging orthometallated phenyl group in **2** now adopts a terminal axial coordination site on Os(3) in **3**. As expected, the phosphorus atoms of the μ_3-$Ph_2PCH_2P(Ph)C_6H_4$ ligand also occupy axial coordination sites to facilitate the coordination of one of the phenyl groups of this ligand to Os(3). The hydride ligand was not located in the X-ray analysis but is believed to bridge across the Os(1)–Os(3) edge which is consistent with the lengthening of this bond and also with the opening out of the CO ligands along this edge {C(2)–Os(1)–Os(3) = 117.65(13) and C(9)–Os(3)–Os(1) = 111.60(14)°}. The Os(3)–C(32) and Os(1)–C(1) bond distances in **3** {2.170(4) and

Table 1
Crystallographic data for **3**, **6**, **8** and **10**

	3	**6**	**8**	**10**
Empirical formula	$C_{41}H_{37}NO_8Os_3P_2$	$C_{39}H_{31}NO_9Os_3P_2$	$C_{22}H_{16}N_2O_9Os_3S$	$C_{39}H_{31}N_2O_8Os_3PS$
Formula weight (Å)	1304.26	1290.19	1055.03	1289.21
Temperature (K)	150(2)	293(2)	150(2)	293(2)
Wavelength (Å)	0.71073	0.71073	0.71073	0.71073
Crystal system	Monoclinic	Triclinic	Monoclinic	Triclinic
Space group	*C*2/*c*	$P\bar{1}$	$P2_1/c$	$P\bar{1}$
Unit cell dimensions				
a (Å)	21.4807(14)	11.388(3)	15.668(4)	15.3857(14)
b (Å)	32.796(2)	11.807(3)	9.122(3)	15.7811(14)
c (Å)	11.7777(8)	14.889(4)	20.026(6)	17.1195(15)
α (°)	90	83.844(4)	90	92.651(2)
β (°)	100.8740(10)	81.697(4)	112.798(4)	102.657(2)
γ (°)	90	89.544(4)	90	101.664(2)
Volume (Å^3)	8148.1(9)	1969.5(8)	2638.5(13)	3954.0(6)
Z	8	2	4	4
Density (calculated) (Mg/m^3)	2.126	2.176	2.656	2.166
Absorption coefficient (mm^{-1})	9.464	9.789	14.543	9.763
F(000)	4896	1204	1912	2408
Crystal size (mm)	0.38 × 0.22 × 0.20	0.28 × 0.12 × 0.08	0.32 × 0.14 × 0.08	0.18 × 0.05 × 0.03
θ Range for data collection (°)	2.48–28.33	2.50–28.28	2.64–28.33	1.22 to 28.29
Index ranges	$-27 \leqslant h \leqslant 27$, $-43 \leqslant k \leqslant 43$, $-15 \leqslant l \leqslant 15$	$-14 \leqslant h \leqslant 15$, $-15 \leqslant k \leqslant 15$, $-19 \leqslant l \leqslant 19$	$-20 \leqslant h \leqslant 20$, $-12 \leqslant k \leqslant 12$, $-26 \leqslant l \leqslant 25$	$-20 \leqslant h \leqslant 20$, $-20 \leqslant k \leqslant 20$, $-22 \leqslant l \leqslant 22$
Reflections collected	34902	17021	21818	34561
Independent reflections	9749 [R_{int} = 0.0378]	9020 [R_{int} = 0.0399]	6290 [R_{int} = 0.0592]	18147 [R_{int} = 0.0523]
Refinement method	Full-matrix least-squares on F^2	Full-matrix least-squares on F^2	Full-matrix least-squares on F^2	Full-matrix least-squares on F^2
Data/restraints/parameters	9749/0/516	9020/0/488	6290/0/339	18147/0/908
Goodness-of-fit on F^2	0.859	0.932	1.094	0.920
Final *R* indices [$I > 2\sigma(I)$]	R_1 = 0.0261, wR_2 = 0.0696	R_1 = 0.0383, wR_2 = 0.0959	R_1 = 0.0411, wR_2 = 0.0983	R_1 = 0.0470, wR_2 = 0.0991
R indices (all data)	R_1 = 0.0314, wR_2 = 0.0727	R_1 = 0.0458, wR_2 = 0.1002	R_1 = 0.0447, wR_2 = 0.1003	R_1 = 0.0800, wR_2 = 0.1225
Largest difference in peak and hole (e Å^{-3})	1.497 and −1.139	3.117 and −1.707	5.399 and −1.925	2.779 and −2.324

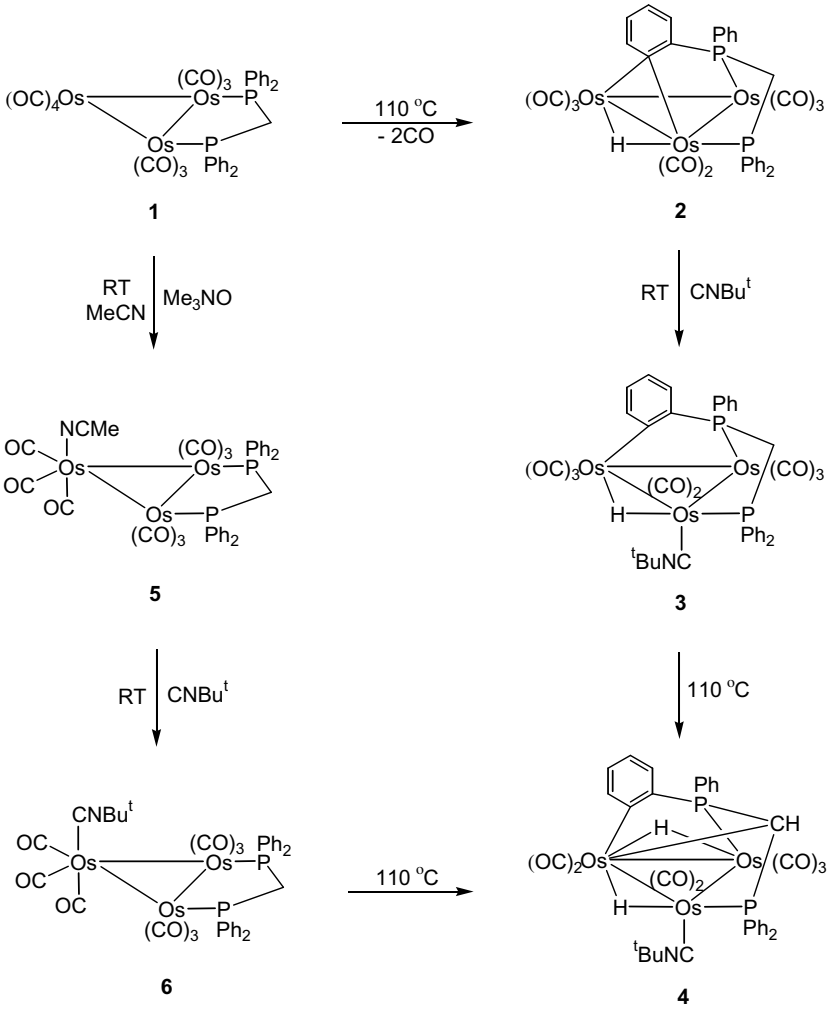

Scheme 3.

2.021(4) Å} are quite similar to those observed in related complexes [10,30] while the Os–P and C–N bond distances are within the range found in literature [11,30–33].

The spectroscopic data for **3** are consistent with the solid-state structure. The infrared spectrum shows the ν_{CN} absorption band at 2178 cm^{-1}, which is characteristic of a terminally coordinated isocyanide ligand [34]. The FAB mass spectrum shows the parent molecular ion peak at *m/z* 1263 and peaks due to sequential loss of eight carbonyl groups. The hydride region of the ^1H NMR spectrum shows a doublet at δ −16.62 (J_{P-H} = 7.6 Hz) indicating the presence of a hydride coupled to a phosphorus atom while the ^{31}P-{^1H} NMR spectrum displays two doublet resonances at δ 12.7 (J_{P-P} = 75.6 Hz,) and 16.5 (J_{P-P} = 75.6 Hz) due to nonequivalent phosphorus atoms of the dppm ligand.

Since we were unable to grow single crystals of **4** in different solvent systems under different conditions, its molecular structure was deduced from spectroscopic data and elemental analysis. The infrared spectrum shows a strong absorption band at 2183 cm^{-1} for the terminally coordinated ^{t}BuNC ligand [34] while the carbonyl region of the spectrum is very similar to that observed for $[Os_3(CO)_7(CNPr)\{\mu_3\text{-}Ph_2PCHP(Ph)C_6H_4\}(\mu\text{-}H)_2]$ [30] which indicates that they have similar distribution of carbonyl ligands. The FAB mass spectrum exhibits the parent molecular ion peak at *m/z* 1235 and peaks due to successive loss of seven carbonyl groups which is consistent with our assigned formulation. The ^1H NMR spectrum of **4** displays two sets of hydride resonances at δ −13.86 and −16.85 indicating that intramolecular activation of two C–H bonds has taken place. In addition to the usual aromatic resonances for phenyl protons, the aliphatic region of the spectrum shows a doublet of doublets at δ 5.10 (J_{P-H} = 11.7, 4.0 Hz) with a relative intensity of 1H for the methylene proton of the dppm ligand and a singlet at δ 1.41 (integrated to 9H) due to the methyl protons of the ^{t}BuNC ligand which suggest that one of the methylene protons of the dppm ligand has been activated. On the other hand, the ^{31}P-{^1H} NMR spectrum shows two doublets at δ −13.7 (J_{P-P} = 53.5 Hz) and −61.8 (J_{P-P} = 53.5 Hz) for the phosphorus atoms of the dppm ligand which is in accord with our proposed structure.

3.2. Reaction of the labile complex $[Os_3(CO)_9(\mu\text{-dppm})(NCMe)]$ (**5**) with ^{t}BuNC

In a related study, we carried out the reaction of the labile acetonitrile complex $[Os_3(CO)_9(\mu\text{-dppm})(NCMe)]$ (**5**) derived from the decacarbonyl compound $[Os_3(CO)_{10}(\mu\text{-dppm})]$ (**1**) with ^{t}BuNC to observe the effect of isocyanide–carbonyl replacement at the unique metal of **1**. Compound **5** reacts with ^{t}BuNC at room temperature to give the simple substitution product $[Os_3(CO)_9$

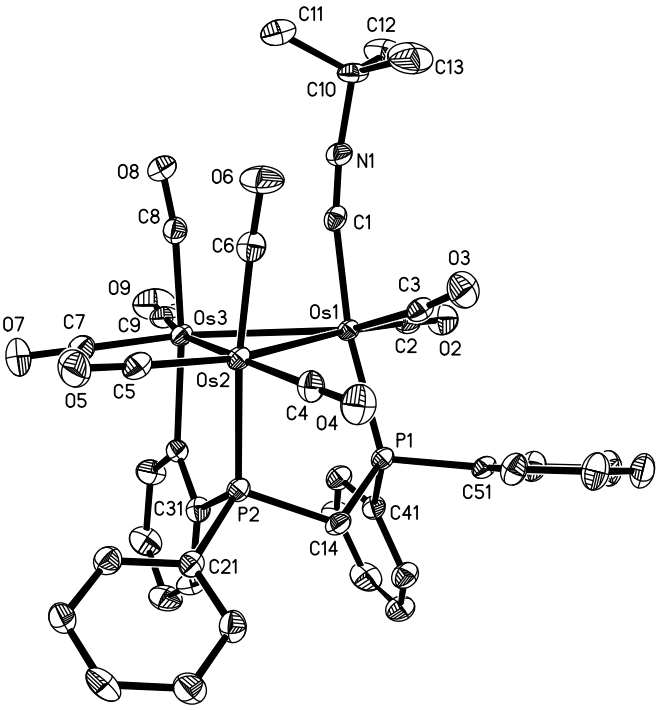

Fig. 1. Molecular structure of $[Os_3(CO)_8\{\mu_3\text{-}Ph_2PCH_2P(Ph)C_6H_4\}(\mu\text{-}H)]$ (**3**) showing 50% probability thermal ellipsoids. Hydrogen atoms are omitted for clarity. Selected bond lengths (Å) and angles(°): Os(1)–Os(2) 2.8961(3), Os(1)–Os(3) 3.0546(3), Os(2)–Os(3) 2.8714(3), Os(1)–C(1) 2.021(4), Os(3)–C(32) 2.170(4), Os(1)–P(1) 2.3837(11), Os(2)–P(2) 2.3575(11), C(1)–N(1) 1.153(5), C(10)–N(1) 1.467(5), C(3)–Os(1)–Os(3) 138.92(13), C(2)–Os(1)–Os(3) 117.65(13), P(1)–Os(1)–Os(2) 89.03(3), Os(2)–Os(1)–Os(3) 57.627(6), Os(3)–Os(2)–Os(1) 63.959(5), Os(2)–Os(3)–Os(1) 58.413(6), P(2)–Os(2)–Os(1) 88.63(3), C(32)–Os(3)–Os(2) 93.69(11), C(9)–Os(3)–Os(1) 111.60(14), C(32)–Os(3)–Os(1) 96.17(11), C(7)–Os(3)–Os(1) 149.69(15), C(8)–Os(3)–Os(1) 88.93(12), P(1)–C(14)–P(2) 107.6(2).

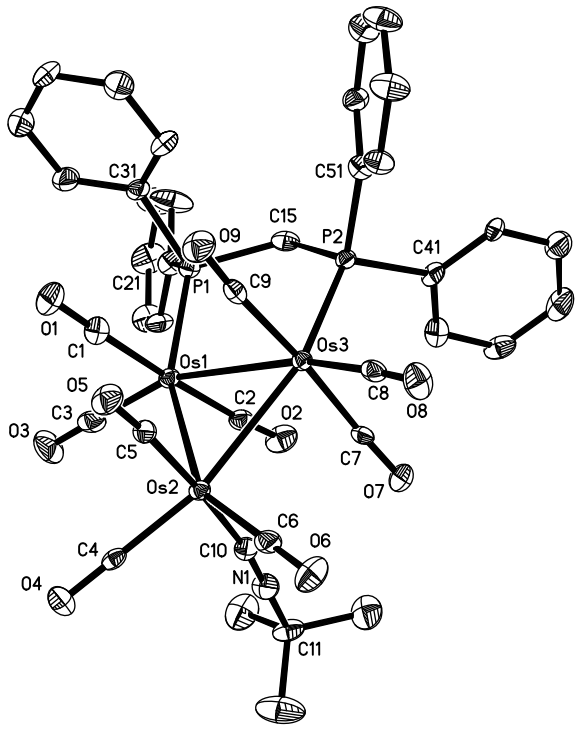

Fig. 2. Molecular structure of $[Os_3(CO)_9(\mu\text{-dppm})(CNBu^t)]$ (**6**) showing 50% probability thermal ellipsoids. Hydrogen atoms are omitted for clarity. Selected bond lengths (Å) and angles (°): Os(1)–Os(2) 2.8514(6), Os(1)–Os(3) 2.8772(6), Os(2)–Os(3) 2.8703(7), Os(2)–C(10) 2.034(6), Os(1)–P(1) 2.3105(17), Os(3)–P(2) 2.3424(17), C(11)–N(1) 1.458(8), C(10)–N(1) 1.149(8), P(1)–Os(1)–Os(3) 92.21(4), P(2)–Os(3)–Os(1) 93.90(4), Os(2)–Os(1)–Os(3) 60.137(18), Os(1)–Os(2)–Os(3) 60.379(14), Os(2)–Os(3)–Os(1) 59.484(10), C(10)–N(1)–N(11) 178.0(7), P(1)–C(15)–P(2) 117.5(4).

(μ-dppm)($CNBu^t$)] (**6**) in which the MeCN group is replaced by the ^{t}BuNC in 51% yield. Decarbonylation of **6** at 110 °C again furnishes **4** in 51% yield (Scheme 3). The structure of compound **6** is similar to the $PhCH_2NC$ analog $[Os_3(CO)_9(CNCH_2Ph)(\mu\text{-dppm})]$ [30]. An ORTEP drawing of the molecular structure of **6** is shown in Fig. 2 and selected bond distances and angles are listed in the caption. The molecule consists of a trimetallic core of three osmium atoms, nine terminal carbonyl groups, a bridging dppm ligand and a terminal ^{t}BuNC ligand. The three osmium atoms form an isosceles triangle with two long {Os(1)–Os(3) = 2.8772(6) and Os(2)–Os(3) = 2.8703(7) Å} and one short {Os(1)–Os(2) = 2.8514(6) Å} metal-metal edge. Each osmium atom is coordinated by three carbonyl ligands and the ^{t}BuNC ligand is axially coordinated to Os(2). The bridging dppm ligand lie in the equatorial plane and the Os–P bond lengths are very similar to those observed in $[Os_3(CO)_9(CNCH_2Ph)(\mu\text{-dppm})]$ [30]. The Os(2)–C(10) bond distance {2.034(6) Å} and the C–N bond distances within the ^{t}BuNC ligand {C(11)–N(1) = 1.458(8), C(10)–N(1) = 1.149(8) Å} are also similar to those found in **3** and $[Os_3(CO)_9(CNCH_2Ph)(\mu\text{-dppm})]$ [30].

The infrared spectrum of compound **6** shows a characteristic absorption band for a terminally coordinated isocyanide ligand at 2178 cm^{-1} [34] while the carbonyl region of the spectrum is very similar to that of $[Os_3(CO)_9(CNCH_2Ph)(\mu\text{-dppm})]$ [30]. In addition to the usual aromatic resonances for phenyl protons, the ^{1}H NMR spectrum shows a multiplet at δ 5.05 for the methylene protons of the dppm ligand while the ^{31}P-{^{1}H} NMR spectrum displays a singlet at δ *−27.3* for the phosphorus atoms of the dppm ligand. The FAB mass spectrum shows the parent molecular ion peak at *m*/*z* 1291 and peaks due to stepwise loss of nine carbonyl ligands which also supports the solid-state structure.

3.3. Reaction of the unsaturated 2-methylbenzothiazole triosmium cluster $[Os_3(CO)_9\{\mu_3\text{-}\eta^2\text{-}C_7H_3(2\text{-}Me)NS\}(\mu\text{-}H)]$ (7) with ^{t}BuNC

The unsaturated cluster $[Os_3(CO)_9\{\mu_3\text{-}\eta^2\text{-}C_7H_3(2\text{-Me})NS\}(\mu\text{-H})]$ (**7**) reacts with ^{t}BuNC at room temperature to furnish the adduct $[Os_3(CO)_9(CNBu^t)\{\mu\text{-}\eta^2\text{-}C_7H_3(2\text{-Me})NS\}(\mu\text{-H})]$ (**8**) which decarbonylates at 110 °C to give unsaturated cluster $[Os_3(CO)_8(CNBu^t)\{\mu_3\text{-}\eta^2\text{-}C_7H_3(2\text{-Me})NS\}(\mu\text{-H})]$ (**9**) (Scheme 4). Compounds **8** and **9** have been characterized by IR, ^{1}H and ^{31}P-{^{1}H} NMR, mass spectroscopy and elemental analysis together with a single crystal X-ray diffraction study for **8**.

An ORTEP drawing of the molecular structure of $[Os_3(CO)_9(CNBu^t)\{\mu\text{-}\eta^2\text{-}C_7H_3(2\text{-Me})NS\}(\mu\text{-H})]$ (**8**) is depicted in Fig. 3 and selected bond distances and angles are listed in the caption. The molecule consists of an isosceles triangle of osmium atoms with one short {Os(1)–Os(3) = 2.8910(7) Å} and two longer bonds {Os(1)–Os(2) = 2.9136(8) and Os(2)–Os(3) = 2.9150(8) Å}, each of which is bonded to three terminal carbonyl groups. The hydride ligand is located crystallographically but not refined. Both the heterocyclic ligand and hydride bridge the same metal–metal edge. The ^{t}BuNC ligand is axially coordinated to Os(1), with the Os(1)–C(10) bond distance {2.039(7) Å} very similar to those found in **3** and **6** and oriented on the opposite side of the Os_3 plane relative to the heterocyclic ligand. The heterocyclic ligand is roughly perpendicular to the Os_3 plane with the C(15)–Os(2)–Os(3) and N(1)–Os(3)–Os(2) angles being 84.52(18) and 84.50(16)°, respectively. The dihedral angle between the Os_3 plane and the mean plane of the heterocyclic ligand is 98.4°. The Os(2)–C(15) and Os(3)–N(1) distances {2.148(7) and 2.174(6) Å} are within the range reported for related compounds [17–22,35–38].

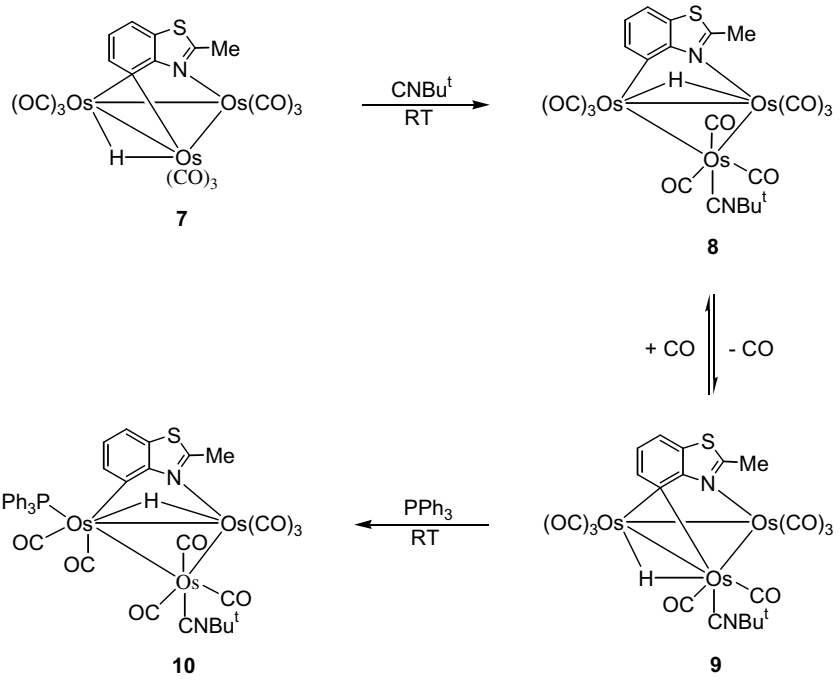

Scheme 4.

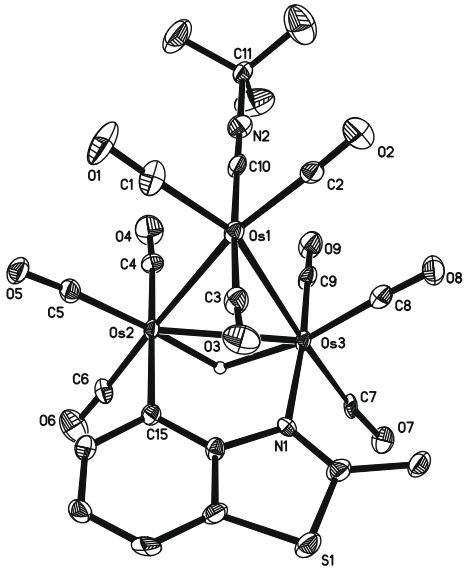

Fig. 3. Molecular structure of $[Os_3(CO)_9(CNBu^t)\{\mu\text{-}\eta^2\text{-}C_7H_3(2\text{-}Me)NS\}(\mu\text{-}H)]$ (**8**) showing 50% probability thermal ellipsoids. Hydrogen atoms are omitted for clarity. Selected bond lengths (Å) and angles (°): Os(1)–Os(2) 2.9136(8), Os(1)–Os(3) 2.8910(7), Os(2)–Os(3) 2.9150(8), Os(1)–C(10) 2.039(7), Os(2)–C(15) 2.148(7), Os(3)–N(1) 2.174(6), C(11)–N(2) 1.453(10), C(10)–N(2) 1.144(10), C(6)–Os(2)–Os(3) 119.0(2), C(15)–Os(2)–Os(3) 84.52(18), C(7)–Os(3)–Os(2) 123.3(2), Os(3)–Os(1)–Os(2) 60.289(17), Os(1)–Os(2)–Os(3) 59.471(10), Os(1)–Os(3)–Os(2) 60.24(2), N(1)–Os(3)–Os(2) 84.50(16), C(10)–N(2)–C(11) 172.6(7).

The ^{1}H NMR spectrum of **8** shows one major isomer (relative intensity = 0.95) in solution with a hydride signal at −11.88. In addition a second hydride resonance is observed at −12.07 (relative intensity = 0.05). The major isomer **8a** is assumed to have the same structure as found in the solid-state, while the minor isomer **8b** has an alternative position for the isocyanide ligand (Chart 1) [27]. The infrared spectrum shows the characteristic ν_{CN} absorption band at 2178 cm^{-1} whereas the FAB mass spectrum exhibits the parent molecular ion peak at m/z 1056 and peaks due to sequential loss of nine carbonyl groups which is consistent with the solid-state structure.

Single crystals of compound **9** could not be obtained after several attempts, so its molecular structure was deduced from elemental analysis and spectroscopic data. The infrared spectrum exhibits the ν_{CN} absorption band at 2164 cm^{-1} which is characteristic of a terminally coordinated isocyanide ligand [34] while the FAB mass spectrum exhibits the parent molecular ion peak at m/z 1028 together with fragment peaks due to successive loss of eight carbonyl groups which is in accord with our proposed formulation. The ^{1}H NMR spectrum exhibits a hydride resonance at δ −12.93 while the aromatic region of the spectrum displays three equal intensity multiplets at δ 8.43, 8.35 and 6.94 due to the ring protons of the heterocylic ligand. In addition to this, the aliphatic region shows two singlets at δ 2.96 and 1.41 with a relative intensity of 1:3 for the methyl protons of the heterocyclic ligand and the ^{t}BuNC ligand respectively which are consistent with our proposed structure.

3.4. Reaction of the unsaturated cluster $[Os_3(CO)_8(CNBu^t)\{\mu_3\text{-}\eta^2\text{-}C_7H_3(2\text{-}Me)NS\}(\mu\text{-}H)]$ (**9**) with CO and PPh_3

The electron deficiency in compound **9** has been demonstrated by its reactions with CO and PPh_3. Treatment of **9** with CO (1 atm)

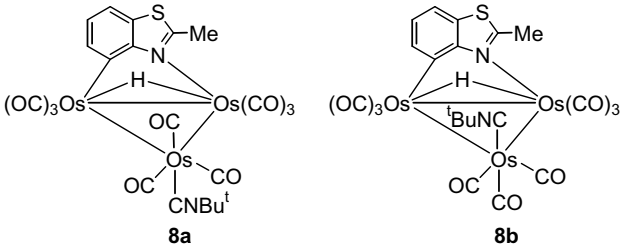

Chart 1.

at room temperature leads to the quantitative formation of **8**. Similarly reaction of **9** with PPh_3 affords the adduct $[Os_3(CO)_8(PPh_3)(CNBu^t)\{\mu\text{-}\eta^2\text{-}C_7H_3(2\text{-}Me)NS(\mu\text{-}H)]$ (**10**) in 56% yield. In order to establish the molecular geometry and in particular to obtain precise details on the disposition of the PPh_3 and the isocyanide ligand, crystal structure analysis of **10** was undertaken. The asymmetric unit contains two chemically indistinguishable molecules and an ORTEP diagram of the molecular structure of one of these is shown in Fig. 4 and selected bond distances and angles are listed in the caption. The structure consists of an irregular triangle of osmium atoms {Os(4)–Os(5) = 2.8723(6), Os(5)–Os(6) = 2.8877(5) and Os(4)–Os(6) = 2.9323(5) Å}, two of which (Os(4) and Os(5)) are coordinated by three carbonyl ligands, while the other, Os(6), is coordinated by two carbonyls. The hydride ligand was not located in the X-ray experiment but from the lengthening of the Os(4)–Os(6) edge, and from the opening out of the carbonyl ligands along this edge {C(11)–Os(4)–Os(6) = 115.8(3)°}, it seems it is likely that it is located on the Os(4)–Os(6) edge. The heterocyclic ligand bridges the same edge, as in **8**, and is almost perpendicular to the Os_3 plane, as shown by the C(60)–Os(6)–Os(5) and N(3)–Os(4)–Os(5) angles of 91.4(2) and 90.2(2)°, respectively. The dihedral angle between the mean plane of the heterocyclic ligand and the plane of the three metal atoms is 85.2°. The ^{t}BuNC ligand is axially coordinated Os(5) and is oriented in the opposite side of the Os_3 plane with respect to the heterocyclic ligand, similarly to **8**. The PPh_3 ligand occupies an equatorial coordination site and is located under the C-7 carbon of the heterocyclic ligand as in related complexes reported in literature [18,19].

The NMR spectrum indicates that compound **10** exists in four isomeric forms in solution (Chart 2) [27,36]. In the ^{1}H NMR spectrum the major isomer **10a** (relative intensity = 0.89) is assumed to have the solid-state structure and shows a hydride signal at δ −11.15 (d, J = 16.4 Hz). In addition, we observe three additional weak hydride resonances at δ −11.35 (d, J = 16.4 Hz), −12.41 (d, J = 16.4 Hz) and −15.20 (d, J = 16.4 Hz) (relative intensity = 0.03, 0.03, 0.05). The equal and relatively large J_{P-H} values are consistent with our proposed structures for the isomers since the phosphine ligand is stereochemically equivalent relative to the hydride in all isomers [36]. The ^{31}P-{^{1}H} NMR spectrum also displays four singlets at δ 12.8, 12.1, 10.0 and 0.5 (relative intensity = 0.05, 0.89, 0.03, 0.03). The infrared spectrum exhibits a strong absorption band at 2178 s cm^{-1} characteristic for terminally coordinated isocyanide ligand while the FAB mass spectrum shows the parent molecular ion peak at m/z 1289 and peaks due to sequential loss of eight terminal carbonyl ligands which are consistent with the solid-state structure.

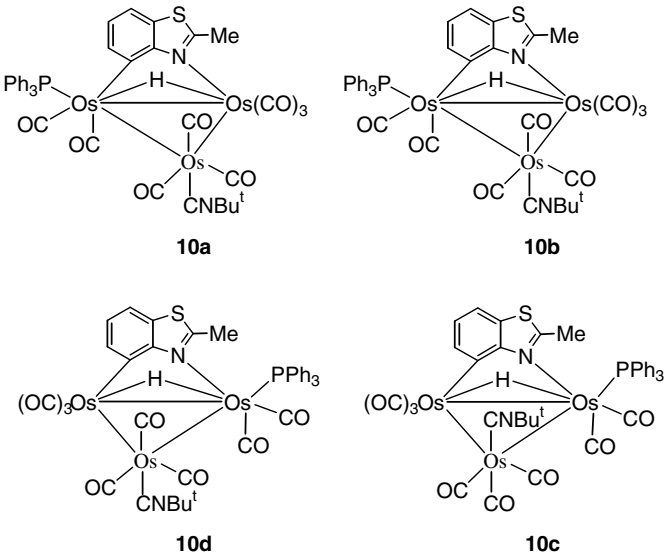

Chart 2.

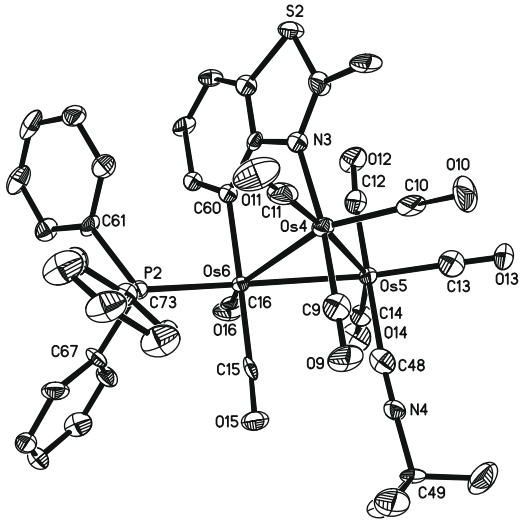

Fig. 4. Molecular structure of $[Os_3(CO)_8(PPh_3)(CNBu^t)\{\mu\text{-}\eta^2\text{-}C_7H_3(2\text{-}Me)NS(\mu\text{-}H)]$ (**10**) showing 50% probability thermal ellipsoids. Hydrogen atoms are omitted for clarity. Selected bond lengths (Å) and angles (°): Os(4)–Os(5) 2.8723(6), Os(5)–Os(6) 2.8877(5), Os(4)–Os(6) 2.9323(5), Os(6)–C(60) 2.161(10), Os(5)–C(48) 2.058(12), Os(6)–P(2) 2.350(2), Os(4)–N(3) 1.169(8), C(48)–N(4) 1.121(13), C(49)–N(4) 1.472(13), Os(5)–Os(4)–Os(6) 59.657(14), Os(4)–Os(5)–Os(6) 61.204(13), Os(5)–Os(6)–Os(4) 59.139(14), P(2)–Os(6)–Os(5) 167.73(6), P(2)–Os(6)–Os(4) 109.48(6), C(11)–Os(4)–Os(6) 115.8(3), N(3)–Os(4)–Os(5) 90.2(2), N(3)–Os(4)–Os(6) 83.9(2), C(48)–Os(5)–Os(4) 91.5(3), C(60)–Os(6)–Os(5) 91.4(2), C(48)–Os(5)–Os(6) 90.5(3), C(48)–N(4)–C(49) 173.3(11), N(4)–C(48)–-Os(5) 171.7(9).

4. Conclusions

In summary, reaction of the unsaturated cluster **2** with ^{t}BuNC gives the adduct **3** which on decarbonylation furnishes the unusual saturated cluster **4** in which both aromatic and aliphatic C–H bond activation has occurred. Similar reaction of the unsaturated cluster **7** with ^{t}BuNC affords the addition product **8** which decarbonylates to give the unsaturated cluster **9**. This difference is difficult to explain in the absence of detailed knowledge of the reaction pathway. Some feature of the substitution of the isocyanide for CO prevents the reformation of a three-center two-electron bond, involving two osmium atoms and the carbon atom of the orthometallated phenyl ring, in **4**. In addition, decarbonylation of **6**, the ^{t}BuNC derivative of the decacarbonyl compound **1**, also furnishes **4**, again pointing to the special impact of this ligand on the formation of the 3-center 2-electron bonding mode. Subsequent reaction of the unsaturated cluster **9** with PPh_3 again affords the saturated cluster **10** in which the phosphine ligand lies under the C-7 carbon of the heterocyclic ligand as in other related unsaturated triosmium clusters [18,19]. Thus, we conclude that isocyanide–carbonyl replacement modifies the chemical behavior of the unsaturated cluster **2** while it has virtually no effect on that of the unsaturated cluster **7**.

Supplementary material

CCDC 655913, 655914, 655915 and 673204 contain supplementary crystallographic data for **3**, **6**, **8** and **10**, respectively. These data may be obtained free of charge from The Cambridge Crystallographic Data Center via www.ccdc.cam.ac.uk/data_request/cif.

Acknowledgements

A. K. R. gratefully acknowledges the University Grants Commission of Bangladesh for a scholarship and the Ministry of Education, Government of the People's Republic of Bangladesh for a study leave.

References

[1] R.D. Adams, H.D. Kaesz, in: D.F. Shriver (Ed.), The Chemistry of Transition Metal Complexes, Wiley, VCH, New York, 1991 (Chapter 4).
[2] G. Lavigne, B. de Bonneval, in: F.A. Cotton (Ed.), Bonneval, Catalysis by Di- and Polynuclear Metal Cluster Complexes, Wiley, VCH, New York, 1998.
[3] A.J. Deeming, Adv. Organomet. Chem. 26 (1986) 1. and references therein.
[4] S.E. Kabir, D.S. Kolwaite, E. Rosenberg, K.I. Hardcastle, W. Cresswell, J. Grindstaff, Organometallics 14 (1995) 3611.
[5] B. Bergman, R. Holmquist, R. Smith, E. Rosenberg, J. Ciurash, K.I. Hardcastle, M. Visi, J. Am. Chem. Soc. 120 (1998) 12818.
[6] E. Rosenberg, S.E. Kabir, M.J. Adedin, K.I. Hardcastle, Organometallics 23 (2004) 3982.
[7] J.A. Clucas, D.F. Foster, M.M. Harding, A.K. Smith, J. Chem. Soc., Chem. Commun. (1984) 949.
[8] J.A. Clucas, M.M. Harding, A.K. Smith, J. Chem. Soc., Chem. Commun. (1985) 1280.
[9] J.A. Clucas, P.A. Dolby, M.M. Harding, A.K. Smith, J. Chem. Soc., Chem. Commun. (1987) 1829.
[10] M.P. Brown, P.A. Dolby, M.M. Harding, A.J. Mathews, A.K. Smith, J. Chem. Soc., Dalton Trans. (1993) 1671.
[11] S.M. Azad, K.A. Azam, S.E. Kabir, M.S. Saha, G.M.G. Hossain, J. Organomet. Chem. 690 (2005) 4206.
[12] A.J. Deeming, M.M. Hassan, S.E. Kabir, E. Nordlander, D.A. Tocher, J. Chem. Soc., Dalton Trans. (2004) 3709.
[13] M.M. Harding, B. Kariuki, A.J. Mathews, A.K. Smith, P. Braunstein, J. Chem. Soc., Dalton Trans. (1994) 33.
[14] S.E. Kabir, A. Miah, L. Nesa, K. Uddin, K.I. Hardcastle, E. Rosenberg, A.J. Deeming, J. Organomet. Chem. 492 (1995) 41.
[15] D.F. Foster, J.H. Harrison, B.S. Nicholls, A.K. Smith, J. Organomet. Chem. 295 (1985) 99.
[16] S. Cartwright, J.A. Clucas, R.H. Dawson, D.F. Foster, M.M. Harding, A.K. Smith, J. Organomet. Chem. 302 (1986) 403.
[17] A.B. Din, B. Bergman, E. Rosenberg, R. Smith, W. Dastru', R. Gobetto, L. Milone, A. Viale, Polyhedron 17 (1998) 2975.
[18] E. Rosenberg, M.J. Abedin, D. Rokhsana, A. Viale, W. Dastru', R. Gobetto, L. Milone, Inorg. Chim. Acta 334 (2002) 343.
[19] E. Arcia, E. Rosenberg, D.S. Kolwaite, K.I. Hardcastle, J. Ciurash, R. Duque, R. Gobetto, L. Milone, D. Osella, M. Botta, W. Dastru', A. Viale, J. Fiedler, Organometallics 17 (1998) 415.
[20] M.J. Abedin, B. Bergman, R. Holmquist, R. Smith, E. Rosenberg, J. Ciurash, K.I. Hardcastle, J. Roe, V. Vazquez, C. Roe, S.E. Kabir, B. Roy, S. Alam, K.A. Azam, Coord. Chem. Rev. 190–192 (1999) 975.
[21] (a) E. Rosenberg, D. Rokhsana, C. Nervi, R. Gobetto, L. Milone, A. Vile, J. Fiedler, M.A. Botavina, J. Organomet. Chem. 23 (2004) 215;
(b) C. Nervi, R. Gobetto, L. Milone, A. Vile, D. Rokhsana, E. Rosenberg, J. Fiedler, Chem. Eur. J. 9 (2003) 5749.
[22] R.D. Adams, N.M. Golembeski, Inorg. Chem. 18 (1979) 1909.
[23] R. Smith, E. Rosenberg, K.I. Hardcastle, V. Vazquez, J. Roh, Organometallics 18 (1999) 3519.
[24] S.E. Kabir, K.M.A. Malik, H.S. Mandal, M.A. Mottalib, M.J. Abedin, E. Rosenberg, Organometallics 21 (2002) 2593.
[25] S.T. Beatty, B. Bergman, E. Rosenberg, W. Dastru', R. Gobetto, L. Milone, A. Vile, J. Organomet. Chem. 593–594 (2000) 226.
[26] N. Begum, A.J. Deeming, M.K. Islam, S.E. Kabir, D. Rokhsana, E. Rosenberg, J. Organomet. Chem. 689 (2004) 2633.
[27] S.R. Hodge, B.F.G. Johnson, J. Lewis, P.R. Raithby, J. Chem. Soc., Dalton Trans. (1987) 931.
[28] SMART and SAINT software for CCD diffractometers, version 6.1, Madison, WI, 2000.
[29] G.M. Sheldrick, SHELXTL PLUS, version 6.1, Bruker AXS, Madison, W1, 2000.
[30] K.-L. Lu, H.-J. Chen, P.-Y. Lu, S.-Y. Li, F.-E. Hong, S.-M. Peng, G.-H. Lee, Organometallics 13 (1994) 585.
[31] M. Day, D. Espitia, K.I. Hardcastle, S.E. kabir, T. McPhillips, E. Rosenberg, Organometallics 12 (1993) 2309.
[32] K.A. Azam, M.B. Hursthouse, M.R. Islam, S.E. Kabir, K.M.A. Malik, R. Miah, C. Sudbrake, H. Varenkamp, J. Chem. Soc., Dalton Trans. (1998) 1097.
[33] N.K.K. Kazemifar, M.J. Stchedroff, M.A. Mottalib, S. Selva, M. Monari, E. Nordlander, Eur. J. Inorg. Chem. (2006) 2058.
[34] R.D. Adams, N.M. Golembeski, J. Am. Chem. Soc. 101 (1979) 2579.
[35] M. Day, D. Espitia, K.I. Hardcastle, S.E. Kabir, T. McPhillips, E. Rosenberg, R. Gobetto, L. Milone, D. Osella, Organometallics 12 (1993) 2309.
[36] M. Day, D. Espitia, K.I. Hardcastle, S.E. Kabir, T. McPhillips, E. Rosenberg, R. Gobetto, L. Milone, D. Osella, Organometallics 10 (1991) 3550.
[37] J. Akter, G.M.G. Hossain, S.E. Kabir, K.M.A. Malik, J. Chem. Crystallogr. 30 (2000) 773.
[38] N. Begum, U.K. Das, G.M.G. Hossain, M.I. Hyder, S.E. Kabir, Indian J. Chem. 44A (2005) 1988.